



Contents lists available at ScienceDirect

Bioorganic & Medicinal Chemistry Letters

journal homepage: www.elsevier.com/locate/bmcl

Design, synthesis, screening, and molecular modeling study of a new series of ROS1 receptor tyrosine kinase inhibitors

Ibrahim M. El-Deeb^b, Byung Sun Park^c, Su Jin Jung^a, Kyung Ho Yoo^a, Chang-Hyun Oh^a, Seung Joo Cho^{d,e}, Dong Keun Han^a, Jae Yeol Lee^c, So Ha Lee^{a,*}

^aLife Sciences Research Division, Korea Institute of Science and Technology, PO Box 131, Cheongryang, Seoul 130-650, Republic of Korea

^bDepartment of Biomolecular Science, University of Science and Technology, 113 Gwahangno, Yuseong-gu, Daejeon 305-333, Republic of Korea

^cResearch Institute for Basic Sciences and Department of Chemistry, College of Science, Kyung Hee University, Seoul 130-701, Republic of Korea

^dResearch Center for Resistant Cells, Chosun University, Gwangju 501-759, Republic of Korea

^eDepartment of Cellular and Molecular Medicine, College of Medicine, Chosun University, 375 Seosuk-dong, Dong-gu Gwangju 501-759, Republic of Korea

ARTICLE INFO

Article history:

Received 2 June 2009

Revised 28 July 2009

Accepted 7 August 2009

Available online 12 August 2009

Keywords:

Kinase inhibitors

ROS1

Glioblastoma multiforme

Homology modeling

Pyrazole

ABSTRACT

A series of rationally designed ROS1 tyrosine kinase inhibitors was synthesized and screened. Compound **12b** has showed good potency with IC₅₀ value of 209 nM, which is comparable with that of the reference lead compound **1**. Molecular modeling studies have been performed, that is, a homology model for ROS1 was built, and the screened inhibitors were docked into its major identified binding site. The docked poses along with the activity data have revealed a group of the essential features for activity. Overall, simplification of the lead compound **1** into compound **12b** has maintained the activity, while facilitated the synthetic advantages. A molecular interaction model for ROS1 kinase and inhibitors has been proposed.

© 2009 Elsevier Ltd. All rights reserved.

The traditional cancer treatments using classical cytotoxic drugs cannot distinguish between normal and cancerous cells, leading to the production of serious side effects, and limiting their long term use in most of cases.^{1,2} These common drawbacks of cytotoxic agents have encouraged scientists to search for more selective and less toxic therapies for different types of cancers. After the new advances in the science of genomics and the characterization of the human genome, the incidence of many types of cancers has been correlated with mutations in genes that confer growth advantage.^{3–5} Among these genes are those encoding for protein kinases, a group of important players in the process of signal transduction that controls normal cell growth and proliferation.^{6,7} Mutations at such genes result usually in the production of the encoded kinases in abnormal high levels and/or constitutive uncontrolled activity, leading to uncontrolled cell proliferation and consequently cancer.^{8–10}

Glioblastoma multiforme is the most advanced astrocytic neoplasm, and is one of the most aggressive human cancers with a median survival of less than one year. Despite decades of therapeutic research, effective chemotherapeutic treatment for high grade astrocytomas is not yet available, and patient care ultimately fo-

cuses on palliative management.^{11–13} In a survey of 45 different human tumor cell lines, the tyrosine kinase ROS1 was found to be expressed in glioblastoma-derived cell lines at high levels, while not expressed at all or expressed minimally in the remaining cell lines.¹⁴ ROS1 kinase is a receptor tyrosine kinase that is homologous to the Drosophila Sevenless tyrosine kinase receptor.^{15–18} It is encoded by ROS1-gene which is located at the chromosome 6 region 6q16 → 6q22. This region is involved in non-random chromosomal arrangements in specific neoplasias.¹⁶ A microdeletion at 6q21 results in the fusion of FIG, a gene coding for a Golgi apparatus-associated protein, to the kinase domain of the proto-oncogene ROS1.^{17,18} The fused protein product FIG-ROS is a potent oncogene, and its transforming potential resides in its ability to interact with and become localized at Golgi apparatus.¹⁷ The ectopic expression of ROS1 receptor protein has been reported mainly in meningiomas and astrocytomas (25% of low grade and 30% of malignant glioma tumors) suggesting a key role for ROS1 kinase in these CNS malignancies.^{17,19} Hence the targeting of the tyrosine kinase ROS1 could be a useful strategy for treatment of astrocytic neoplasms.

In a previous work reported by our group²⁰, a new potent and highly selective ROS1 kinase inhibitor **1** was synthesized and evaluated (Fig. 1). The synthesized compound **1** was screened over 45 different kinases, and showed a high selectivity towards ROS1

* Corresponding author. Tel.: +82 2 958 6834; fax: +82 2 958 5189.

E-mail address: LSH6211@kist.re.kr (S.H. Lee).

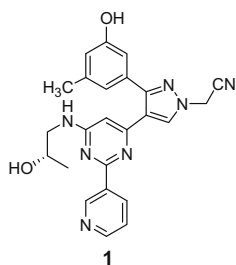
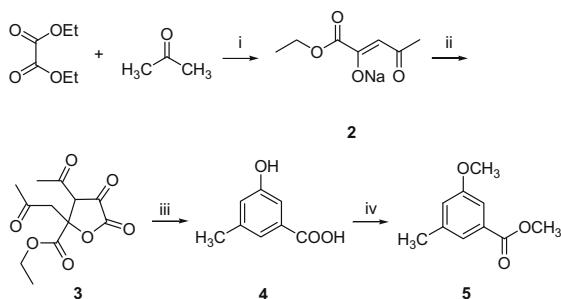


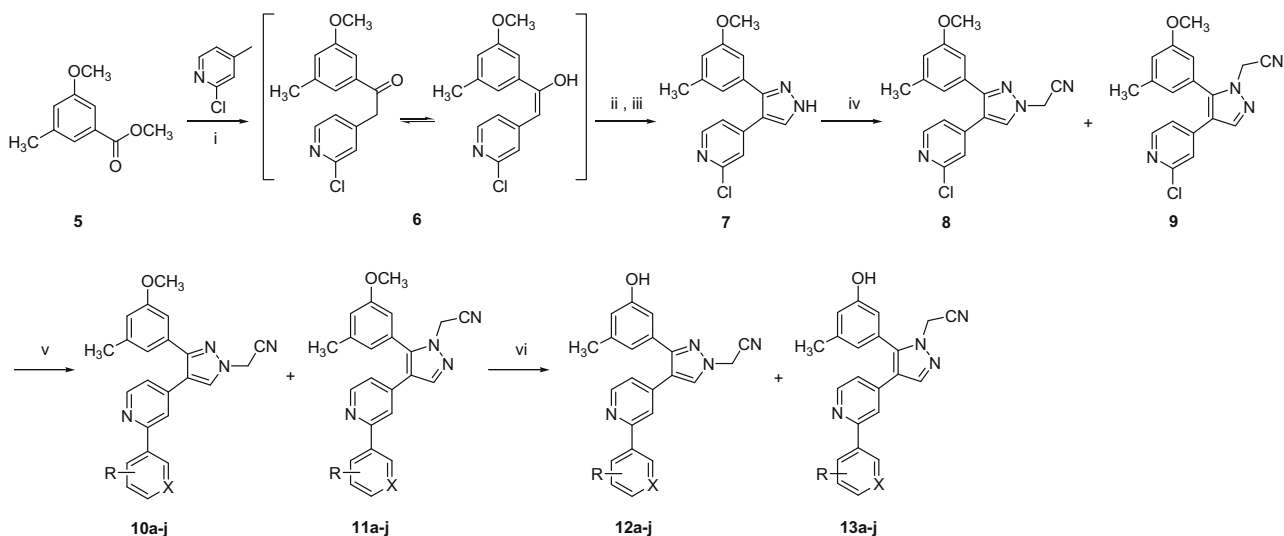
Figure 1. Structure of the lead compound **1**.

kinase, associated with good potency ($IC_{50} = 199$ nM). In this Letter, a series of rationally designed compounds have been synthesized and screened over ROS1 kinase in order to study the structure–activity relationship for this new class of inhibitors. A molecular modeling study was also made in order to get a better molecular insight on the mode of enzyme inhibition of these inhibitors, where a homology model for the enzyme ROS1 was built, and the tested compounds were docked into the potential binding site of the built homology.

The synthesis work started with the preparation of the key ester, methyl 3-methoxy-5-methylbenzoate (**5**) as illustrated in Scheme 1. In the first step, the sodium salt of ethyl 2-hydroxy-4-oxopent-2-enoate (**2**) was prepared according to literature proce-



Scheme 1. Reaction conditions and reagents: (i) NaOEt, abs EtOH, rt, 4 h, 87%; (ii) acetic acid: H₂O (1:1), rt, 2 h, 50%; (iii) MgO, H₂O, reflux, 45 min, 42%; (iv) K₂CO₃, CH₃I, DMAP, acetone, 65 °C, 12 h, 94%.



Scheme 2. Reaction conditions and yields: (i) LHMDS, THF, N₂, rt, 18 h, 72%; (ii) DMF–DMA, reflux, 12 h; (iii) hydrazine hydrate, abs EtOH, rt, 2 h, 81%; (iv) K₂CO₃, iodoacetonitrile, acetone, reflux, 4 h, 92%; (v) arylboronic acid, Pd(PPh₃)₂Cl₂, Na₂CO₃, N₂, THF/H₂O (4:1), 70 °C, 12 h; (vi) BF₃·S(CH₃)₂, dichloromethane, N₂, rt, 24 h.

dures²¹, through the condensation of diethyl oxalate with acetone in the presence of sodium ethoxide in absolute ethanol. The resulted salt **2** was then cyclized into Claisen furan derivative **3** by heating in 50% acetic acid followed by acidification with sulfuric acid.²² The resulted Claisen compound underwent rearrangement and aromatization into 3-hydroxy-5-methylbenzoic acid (**4**) within less than one hour by heating with magnesium oxide in boiling water, followed by acidification with hydrochloric acid to precipitate the free acid.²²

Methyl esterification and O-methylation of the resulted phenolic acid **4** were achieved in a single step and in a high yield (94%) to give compound **5** through a little modification of the literature procedure,²³ where the acid **4** was refluxed with excess potassium carbonate and iodomethane in acetone, and in the presence of a catalytic amount of DMAP.

In Scheme 2, the benzoate ester **5** underwent a nucleophilic attack at its carboxylic carbon by the activated methylene group of 2-chloro-4-methylpyrimidine. The activation of this methyl group into an active methylene was achieved by dropwise addition of lithium bis(trimethylsilyl)amide (LHMDS) in dry THF at room temperature. The resulted tautomeric α,β -unsaturated ketone **6** was then converted to the required pyrazole derivative **7** through two successive steps. In the first step, compound **6** was heated with excess *N,N*-dimethylformamide dimethylacetal for 12 h, and the resulted product was taken to the next step without further purification, where it was cyclized with hydrazine monohydrate in absolute ethanol into the pyrazole derivative **7**. The reaction of the resulted pyrazole **7** with iodoacetonitrile in the presence of excess potassium carbonate produced two different regioisomers; a major isomer **8** with *R_f* value of 0.74 (EtOAc–hexane 1:1 v/v), and a minor isomer **9** with *R_f* value of 0.84 (EtOAc–hexane 1:1 v/v). A mixture of these two isomers was taken to the next step without separation, where it underwent a Suzuki coupling with a series of arylboronic acids, in the presence of dichloro-bis(triphenylphosphine) Pd(II) and potassium carbonate, in a mixed solvent of THF and water in a (4:1) ratio. These series of Suzuki coupling reactions produced two isomers in every reaction **10a–j** and **11a–j**, which were separated in a pure form by preparative TLC. In all of these reactions, the 1*H*-pyrazole isomer (isomer **10**) was the product with the lower *R_f* value while the 2*H*-pyrazole isomer (isomer **11**) was the product with the higher *R_f*. This was proved by the 2D-NOESY NMR spectrum of compounds **10h** and **11h** as a model for

the whole series. The absence of any cross peaks between the acetonitrile $-\text{CH}_2-$ and any of the aromatic protons of 3-methoxy-5-methylphenyl group in the 2D-NOESY NMR spectrum of compound **10h** while the presence of such peaks in the 2D-NOESY NMR spectrum of compound **11h** has confirmed the assigned structures. The final hydroxyl derivatives **12a–j** and **13a–j** were obtained by demethylation of the methoxy group of the corresponding methoxy compounds using 10 equiv of borontrifluoride–dimethylsulfide complex in dichloromethane.

In Scheme 3, typical procedures to those used in Scheme 2 have been applied. The only difference was in the starting amine, where in Scheme 3 and 2-chloro-5-methylpyridine was used instead of 2-chloro-4-methyl-pyridine (Table 1).

Kinase assays were performed at Reaction Biology Corporation using the 'HotSpot' assay platform.²⁴ In the initial screening step; the 14 selected compounds showed in Figure 2 were tested over ROS1 kinase at a single dose of 20 μM , and the reaction was carried out at 10 μM ATP concentration. At this concentration, compound **12b** showed a significant inhibition of 96% for the activity of ROS1 kinase, while the inhibition exerted by all of the other tested compounds was below 30%. Accordingly, compound **12b** was further tested in a 10-dose IC_{50} mode with threefold serial dilutions starting at 20 μM . Staurosporine²⁵ was used as a control compound in a 10-dose IC_{50} mode with fivefold serial dilutions starting at 20 μM , and the reaction was carried out at 10 μM ATP concentration. The new compound **12b** has showed an IC_{50} value of 209 nM which is comparable with that of the reference compound **1** (Fig. 2).

In order to apply a molecular modeling study for the tested derivatives and correlate between their activities and their binding mode to the enzyme, a homology model for ROS1 kinase was built using MOE software (2008.10 version). The last 1347 amino acids of the total 2347 residues of ROS1 which are predicted to contain the kinase domain of the enzyme^{26–28} were used to build the homology model over the 3D crystal structure of the insulin-like growth factor-1 receptor kinase (PDB code 1P4O).

A good homology between the two proteins was predicted with E value of $1.4\text{e-}57$. The sequences of the two proteins were aligned and the built homolog was relaxed applying force field Amber99 calculations.²⁷ The site identifier has identified a major binding site made up of 28 residues and having a size of 172 Å. The docking results for the reference compound **1** and compound **12b** have revealed that both of the two compounds have the same pose that occupies the same space inside the binding pocket (Fig. 3).

In this binding pose, the compound is fit into the receptor site through four hydrogen bonds. Two hydrogen bonds between the

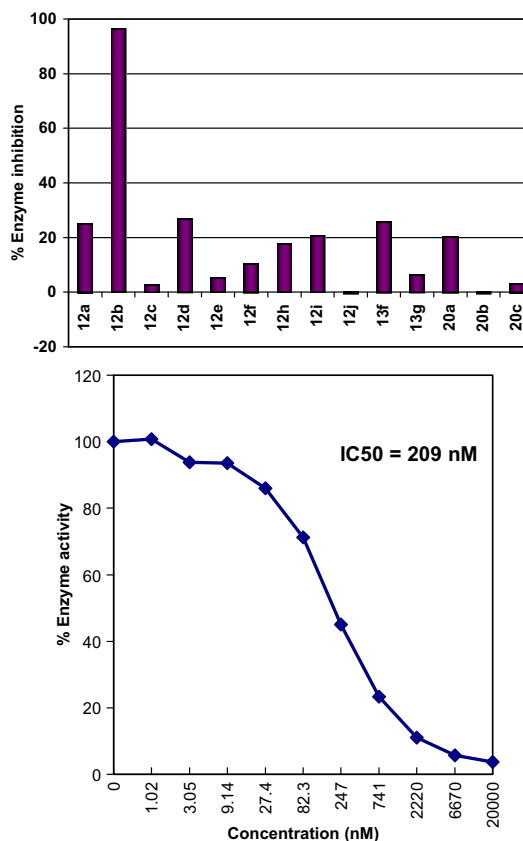
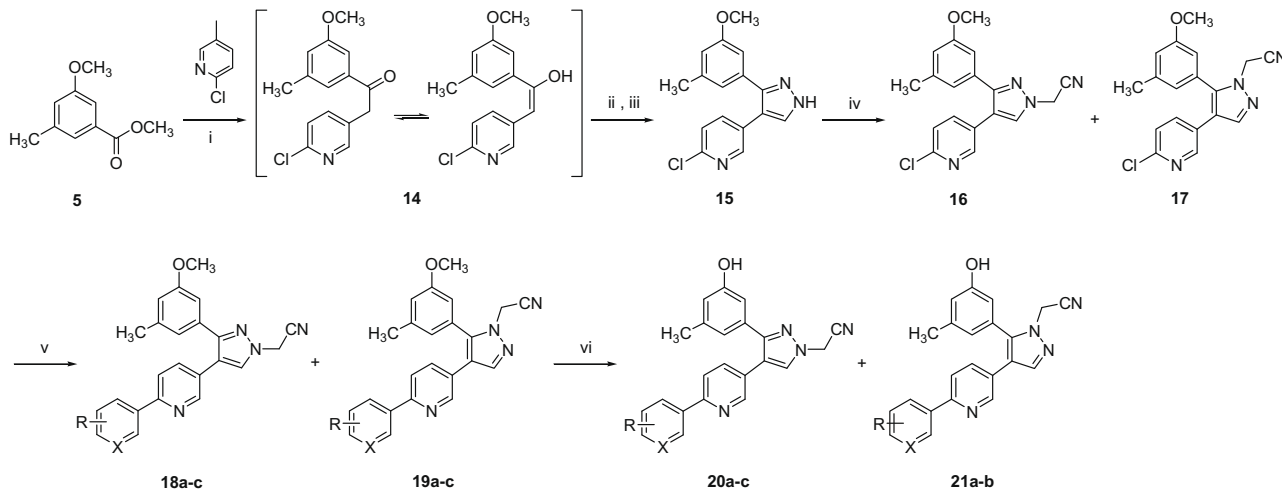


Figure 2. % of ROS1 enzyme inhibition exerted by single dose concentration of 20 μM (upper panel), dose–activity curve for compound **12b** on ROS1 kinase (lower panel).

acetonitrile nitrogen and leucine 1105 and alanine 1106, one hydrogen bond between the phenolic OH and leucine 1122, and a fourth hydrogen bond between the terminal pyridyl nitrogen and lysine 1111 (Fig. 4).²⁹

By investigating the binding interactions of the reference compound **1** (Fig. 3), it was found that the pyrimidinyl nitrogens do not share in any hydrogen bonding in the receptor. In addition, the 1-aminopropan-2-ol group does not support any significant binding for the compound in the receptor site. These observations were consistent with the screening results for the two active compounds



Scheme 3. Reaction conditions and yields: (i) LHMDS, THF, N_2 , rt, 18 h, 55%; (ii) DMF–DMA, reflux, 12 h; (iii) hydrazine hydrate, abs EtOH, rt, 4 h, 62%; (iv) K_2CO_3 , iodoacetone, acetone, reflux, 4 h, 80%; (v) arylboronic acid, $\text{Pd}(\text{PPh}_3)_2\text{Cl}_2$, Na_2CO_3 , N_2 , THF/ H_2O (4:1), 70 $^\circ\text{C}$, 12 h; (vi) $\text{BF}_3 \cdot \text{S}(\text{CH}_3)_2$, dichloromethane, N_2 , rt, 24 h.

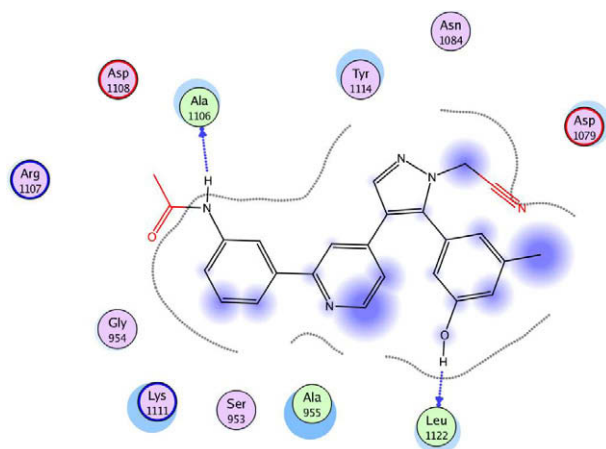


Figure 5. Proposed clash between compound **13g** and the receptor surface when occupy the same pose of compound **12b**.

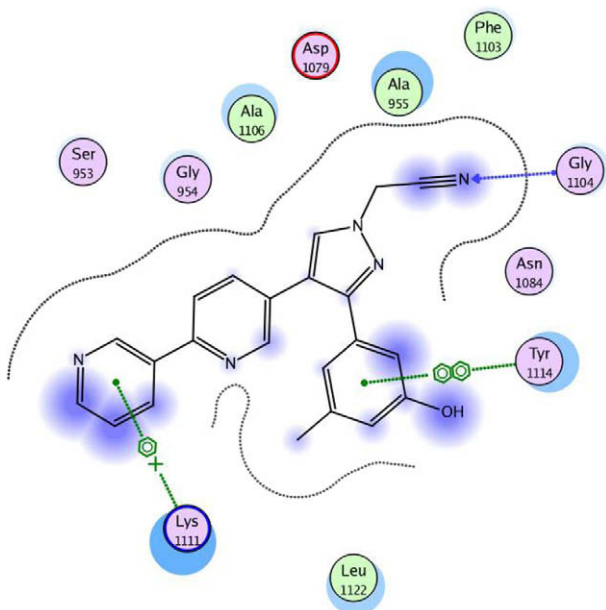


Figure 6. Binding mode of compound **20a**.

together, and a barcode presentation mode was established to view all the interacting residues against the docked compounds, and the characteristic bindings with each of them. As showed in Figure 7, a unique common binding feature in compounds **1** and **12b** is the binding with leucine 1122. This characteristic binding was not observed at any of the other derivatives. This figure reveals also that

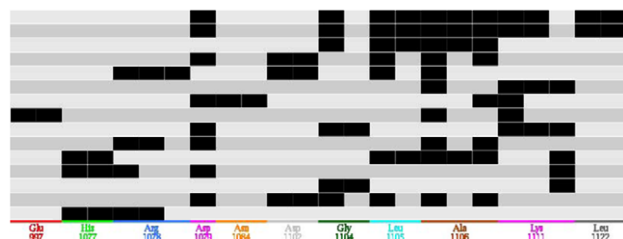


Figure 7. Barcode presentation mode for the characteristic interactions of the screened compounds at the receptor site (the order from top to bottom: **1**, **12b**, **12a**, **12c**, **12d**, **12e**, **12f**, **13f**, **13g**, **12h**, **12i**, **12j**, **20a**, **20b**, **20c**).

these two active compounds (**1** and **12b**) have typical binding profiles, which accounts for their identical inhibitory activity.

In conclusion, the molecular modeling study has showed that the more simple structure of compound **12b** contains three essential features for activity (terminal pyridyl, 1*H*-acetonitrile, and phenolic hydroxyl), and that this structure is highly conserved in most of its parts. A possible site that is yet viable for more modifications is the methyl group at the 3-hydroxy-5-methylphenyl ring. The extension of structure originated from this point may produce derivatives with extending binding features and possible enhancement in activity.

Acknowledgments

This research was supported by Korea Institute of Science and Technology and Pioneer Research Program for converging technology through the Korea Science and Engineering Foundation funded by the Ministry of Education, Science and Technology (M10711060001-08M1106-00110). We also appreciate to Dr. Sean W. Deacon and Dr. Haiching Ma from Reaction Biology Corporation for kinase screening.

References and notes

- Hirsch, J. *JAMA* **2006**, *296*, 1518.
- Lewis, L. D. *Br. J. Clin. Pharmacol.* **2006**, *62*, 1.
- Buchanan, G.; Greenberg, N. M.; Scher, H. I.; Harris, J. M.; Marshall, V. R.; Tilley, W. D. *Clin. Cancer Res.* **2001**, *7*, 1273.
- Soussi, T.; Beroud, C. *Hum. Mutat.* **2003**, *21*, 192.
- Dorak, M. T.; Burnett, A. K.; Worwood, M. *Genet. Med.* **2005**, *7*, 159.
- Chase, A.; Cross, N. C. P. *Clin. Sci.* **2006**, *111*, 233.
- Missner, E.; Bahr, I.; Badock, V.; Lucking, U.; Siemeister, G.; Donner, P. *Chembiochem* **2009**, *10*, 1163.
- Chalandon, Y.; Schwaller, J. *Haematologica* **2005**, *90*, 949.
- Lengyel, E.; Sawada, K.; Salgia, R. *Curr. Mol. Med.* **2007**, *7*, 77.
- Sardon, T.; Cottin, T.; Xu, J.; Giannis, A.; Vernos, I. *Chembiochem* **2009**, *10*, 464.
- Holland, E. C. *Proc. Natl. Acad. Sci. U.S.A.* **2000**, *97*, 6242.
- Hess, S. M.; Anderson, J. G.; Bierbach, U. *Bioorg. Med. Chem. Lett.* **2005**, *15*, 443.
- Ohgaki, H.; Kleihues, P. *Am. J. Pathol.* **2007**, *170*, 1445.
- Birchmeier, C.; Sharma, S.; Wigler, M. *Proc. Natl. Acad. Sci. U.S.A.* **1987**, *84*, 9270.
- Tessarollo, L.; Nagarajan, L.; Parada, L. F. *Development* **1992**, *115*, 11.
- Nagarajan, L.; Louie, E.; Tsujimoto, Y.; Balduzzi, P. C.; Huebner, K.; Croce, C. M. *Proc. Natl. Acad. Sci. U.S.A.* **1986**, *83*, 6568.
- Charest, A.; Kheifets, V.; Park, J.; Lane, K.; McMahon, K.; Nutt, C. L.; Housman, D. *Proc. Natl. Acad. Sci. U.S.A.* **2003**, *100*, 916.
- Charest, A.; Lane, K.; McMahon, K.; Park, J.; Preisinger, E.; Conroy, H.; Housman, D. *Gene Chromosome. Canc.* **2003**, *37*, 58.
- Jun, H. J.; Woolfenden, S.; Coven, S.; Lane, K.; Bronson, R.; Housman, D.; Charest, A. *Cancer Res.* **2009**, *69*, 2180.
- Park, B. S.; El-Deeb, I. M.; Yoo, K. H.; Oh, C. H.; Cho, S. J.; Han, D. K.; Lee, H. S.; Lee, J. Y.; Lee, S. H. *Bioorg. Med. Chem. Lett.* **2009**, *19*, 4720.
- Wipf, P.; Mahler, S. G.; Okumura, K. *Org. Lett.* **2005**, *7*, 4483.
- Turner, F. A.; Gearien, J. E. *J. Org. Chem.* **1959**, *24*, 1952.
- De Frutos, O.; Atienza, C.; Echavarren, A. M. *Eur. J. Org. Chem.* **2001**, *1*, 163.
- Kinase assays were performed at Reaction Biology Corporation using the 'HotSpot' assay platform. Kinase Assay Protocol: Reaction Buffer: 20 mM Hepes (pH 7.5), 10 mM MgCl₂, 1 mM EGTA, 0.02% Brij35, 0.02 mg/ml BSA, 0.1 mM Na₃VO₄, 2 mM DTT, 1% DMSO. Reaction Procedure: To a freshly prepared buffer solution was added ROS1 kinase at a concentration of 20 μM. The contents were mixed gently, then the compound under test dissolved in DMSO was added to the reaction mixture in the appropriate concentration. 339-ATP (specific activity 500 μCi/μl) was added to the mixture in order to initiate the reaction, and the mixture was incubated at room temperature for 2 h. Initial single dose screening: The compound was tested by single dose duplicate made at a concentration of 10 μM. Staurosporine was used as a control compound in a 5-dose IC₅₀ mode with 10-fold serial dilutions starting at 20 μM. Reaction was carried out at 10 μM ATP concentration. Testing in IC₅₀ mode: Compound **12b** was tested in a 10-dose IC₅₀ mode with threefold serial dilutions starting at 20 μM. Staurosporine was used as a control compound in a 10-dose IC₅₀ mode with fivefold serial dilutions starting at 20 μM. Reaction was carried out at 10 μM ATP concentration.
- Yang, S.; Malaviya, R.; Wilson, L. J.; Argenti, R.; Chen, X.; Yang, C.; Wang, B.; Cavender, D.; Murray, W. V. *Bioorg. Med. Chem. Lett.* **2007**, *17*, 326.
- Birchmeier, C.; Birnbaum, D.; Waitches, G.; Fasano, O.; Weigler, M. *Mol. Cell Biol.* **1986**, *6*, 3109.
- Birchmeier, C.; O'Neill, K.; Riggs, M.; Wigler, M. *Proc. Natl. Acad. Sci. U.S.A.* **1990**, *87*, 4799.
- Wang, J.; Cieplik, P.; Kollman, P. A. *J. Comput. Chem.* **2001**, *21*, 1049.
- The showed residues' numbers refer to the amino acid sequence in the built model which is 1000 less than the actual number in the whole original protein.